CHAPTER V

Influence of gold nanoparticles concentrations on polymer functionalized reduced graphene oxide nanosheets and its electrochemical sensing performance

CHAPTER V

INFLUENCE OF GOLD NANOPARTICLES CONCENTRATION ON POLYMER FUNCTIONALIZED REDUCED GRAPHENE OXIDE NANOSHEETS AND ITS ELECTROCHEMICAL SENSING PERFORMANCE

This chapter includes:

- Introduction
- Materials and methods
- Functional and Structural characterization of various concentrations of rGONS/β-CD/Au nanocomposite
- Morphological analysis
- Elemental analysis
- Electrocatalytic analysis for the sensing of nitrophenol isomers
- Conclusion
- References

5.1. INTRODUCTION

Electrochemical sensor is a versatile and inexpensive method for the detection of analytes from environment and it is frequently used for the detection of wide range of harmful and biological compounds [1]. In electrochemical sensing technology, the reduction and oxidation mechanism of the analytes are strongly depend on the concentration of the nanocomposite used to modify the electrode surface, electrolyte pH and scan rate [2-3]. In this chapter, the influence of gold nanoparticles concentration on the morphology, structural and electrochemical properties of β-cyclodextrin functionalized reduced graphene oxide nanosheet is discussed. The electrochemical sensing properties of the different concentrations of the rGONS/β-CD/Au nanocomposites towards the detection of nitrophenol isomers are also discussed in aqueous electrolyte solutions. Nitrophenols (NPs) are highly toxic organic compounds

commonly used in the manufacturing of pesticides, dyes, pharmaceuticals and explosives [4]. The nitrophenol isomers such as ortho nitrophenol (o-NP), para nitrophenol (p-NP) and meta-nitrophenol (m-NP) have momentous toxic effects on human beings, mammals, microorganisms and plants. Hence, the detection of nitrophenols is of extreme importance, since it is noticed as pollution abatement [5].

5.2. MATERIALS AND METHODS

The graphene oxide nanopowder (GO) is prepared by the modified Hummer's method [6-7]. The β-cyclodextrin molecules functionalized reduced graphene oxide (rGO/β-CD) nanosheets are synthesized by taking 50 ml aqueous solution containing 0.6 g of β-cyclodextrin polymer that are mixed with the 50 ml of dispersed graphene oxide suspension followed by the addition of ammonia solution and hydrazine hydrate (80 wt%) as a reducing and stabilizing agents. The reaction mixture is then stirred at 60˚C for 4 hrs and centrifuged using deionized water [8-9]. The gold nanoparticles are decorated on the surface of rGONS/β-CD nanosheets by taking the dispersed rGONS/ β-CD reaction suspension followed by the addition of 100 ml of 0.002 M concentration of gold (III) chloride trihydrate solution. The dispersed 0.005 M concentration solution of sodium borohydrate is added into the above reaction mixture to reduce gold (III) chloride trihydrate into gold nanoparticles. The reaction suspension is then stirred for 4 hours at 80˚C and centrifuged using deionized water. To get as fine powder of gold nanoparticles encapsulated rGONS/β-CD nanosheets, the rGONS/β-CD/Au reaction suspension is dried at 60˚C for 4 hours [9]. The similar synthesis procedure is repeated for the synthesis of various concentrations (0.004 M, 0.006 M, 0.008 M and 0.01 M) of gold (III) chloride trihydrate.

5.3. RESULTS AND DISCUSSION

5.3.1. FT-IR SPECTRAL ANALYSIS

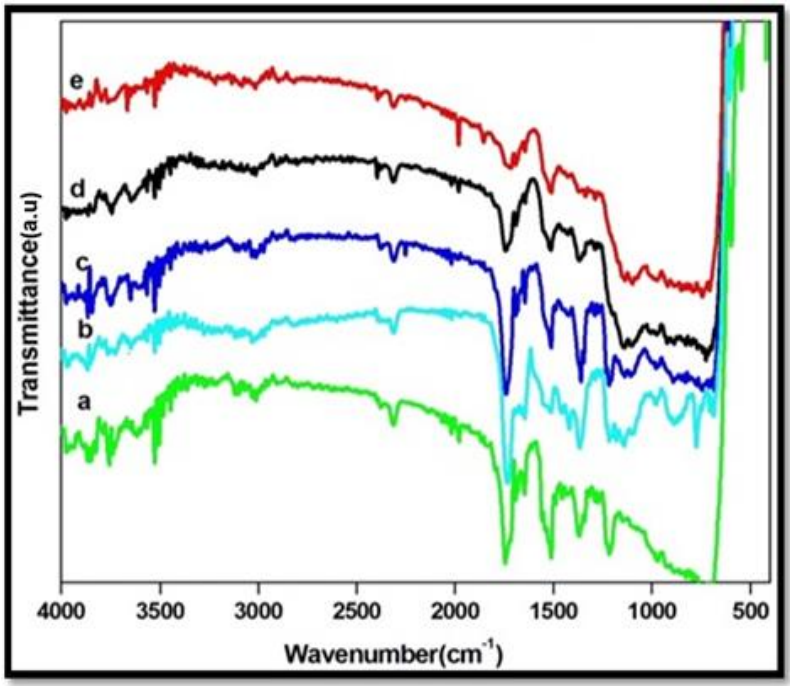

Figure.5.1. FT-IR spectra of gold nanoparticles encapsulated β-cyclodextrin functionalized reduced graphene oxide nanosheets using (a) 0.002 M (b) 0.004 M (c) 0.006 M (d) 0.008 M (e) 0.01 M concentrations of gold (III) chloride trihydrate

Figure.5.1.(a-e) shows the Fourier transform infrared (FT-IR) spectra of different concentrations (0.002 M, 0.004 M, 0.006 M, 0.008 M and 0.01 M) of gold nanoparticles encapsulated β-cyclodextrin polymer functionalized reduced graphene oxide nanosheets (rGONS/β-CD/Au). The FT-IR bands observed at 1218 cm^{-1}, 1366 cm^{-1}, 1514 cm^{-1} and 3520 cm^{-1} are corresponding to the stretching vibration of C-O, C-OH, C=C and O-H groups of reduced graphene oxide nanosheets respectively [10]. The bands obtained around 28985.42 cm^{-1}, 2309 cm^{-1} and 3765 cm^{-1} may be attributed to the CH_2 bending, CH_2 and O-H stretching vibrations of β-CD polymer [11-12]. The band that appeared between 400 cm^{-1} to 1000 cm^{-1} may correspond to the presence of gold nanoparticles encapsulated on the surface of rGONS/β-CD nanosheets.

It is observed from the Figure.5.1.(a-e) that the FT-IR bands corresponding to the hydroxyl groups of reduced graphene oxide nanosheets are shifted towards the higher wave number and which may be due to the intermolecular interactions between

the oxygen functional groups of reduced graphene oxide nanosheets with β-cyclodextrin polymer. This shift further confirms the functionalization and encapsulation of β-cyclodextrin and gold nanoparticles on the surface of reduced graphene oxide nanosheets [11] [13] [8]. It is also observed from the FT-IR spectra that the depth of the band of carbon-oxygen functional groups (C-O, O-H and C-H) of reduced graphene oxide nanosheets and β-CD polymer decreases gradually with the increase in the concentration of gold (III) chloride trihydrate from 0.002 M to 0.01 M, which confirms the influence of gold nanoparticles concentration on the surface of rGONS/β-CD nanosheets.

5.3.2. STRUCTURAL ANALYSIS

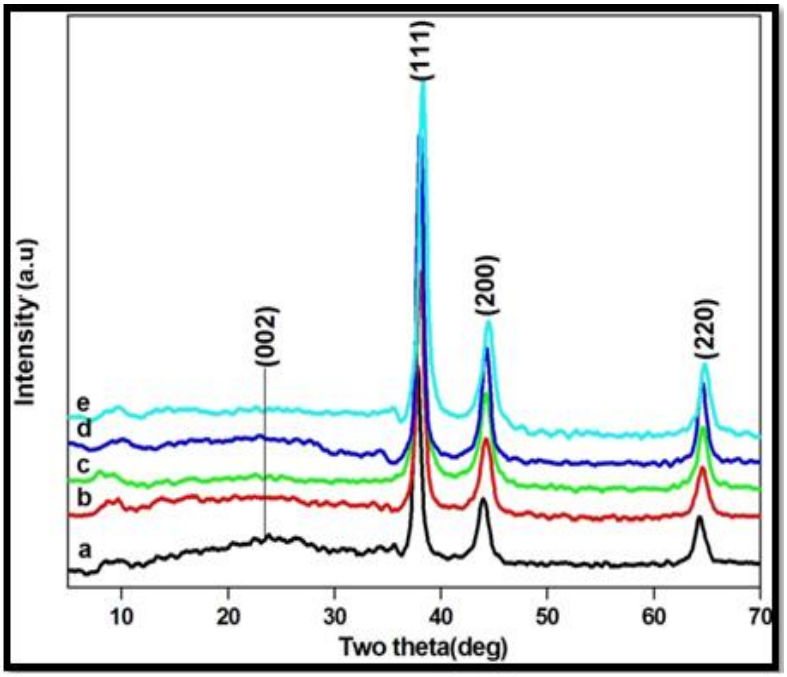

Figure.5.2. XRD spectra of gold nanoparticles encapsulated β-cyclodextrin functionalized reduced graphene oxide nanosheets using (a) 0.002 M (b) 0.004 M (c) 0.006 M (d) 0.008 M and (e) 0.01 M concentration of gold (III) chloride trihydrate

The X-ray diffraction analysis is used to study the crystalline and phase structure of the synthesized samples. Figure.5.2.(a-e) shows the XRD pattern of various concentrations (0.002 M, 0.004 M, 0.006 M, 0.008 M, 0.01 M) of gold nanoparticles encapsulated β-cyclodextrin functionalized reduced graphene oxide nanosheets. It is observed from the Figure.5.2.(a-e) that the diffraction peaks obtained at the angle of

38.02˚, 44.2˚ and 64.06˚ can be indexed to the (111), (200) and (220) reflection planes of the face centered cubic (fcc) structure of gold nanoparticles respectively and are well matched with the JCPDS card number (004-0784) [14-15].

The crystallite size of the gold nanoparticles can be calculated using the Debye-Scherrer equation [16] and are 9.20 nm, 9.19 nm, 9.16 nm, 9.91 nm and 12.62 nm for the different concentrations (0.002 M, 0.004 M, 0.006 M, 0.008 M, 0.01M) of gold nanoparticles encapsulated on the surface of rGONS/β-CD nanosheets respectively. The crystallite size of the gold nanoparticles encapsulated on the surface of rGONS/CD surface is found to dramatically increase for the concentration of 0.008 M and 0.01 M of gold (III) chloride trihydrate and this may be due to the aggregation of gold nanoparticles, which could also be evidenced from SEM analysis. It is further observed from the Figure.5.2.(a-e) that the intensity of the diffraction peak corresponding to the gold nanoparticles increases with the increase in its concentration from 0.002 M to 0.01 M, which confirms the presence and uniform decoration of high crystalline gold nanoparticles on the surface of rGO/β-CD nanosheets. In the XRD spectra of rGONS/β-CD/Au nanocomposite, the diffraction peak appeared at 24.3˚ with the crystalline plane of (002) of rGO/β-CD nanosheet decreases with the increase in the concentration of gold chloride trihydrate from 0.002 M to 0.01 M, which confirms the influence of gold nanoparticles concentrations on the structural property of rGO/β-CD/Au nanocomposites [14].

5.3.3. SEM ANALYSIS

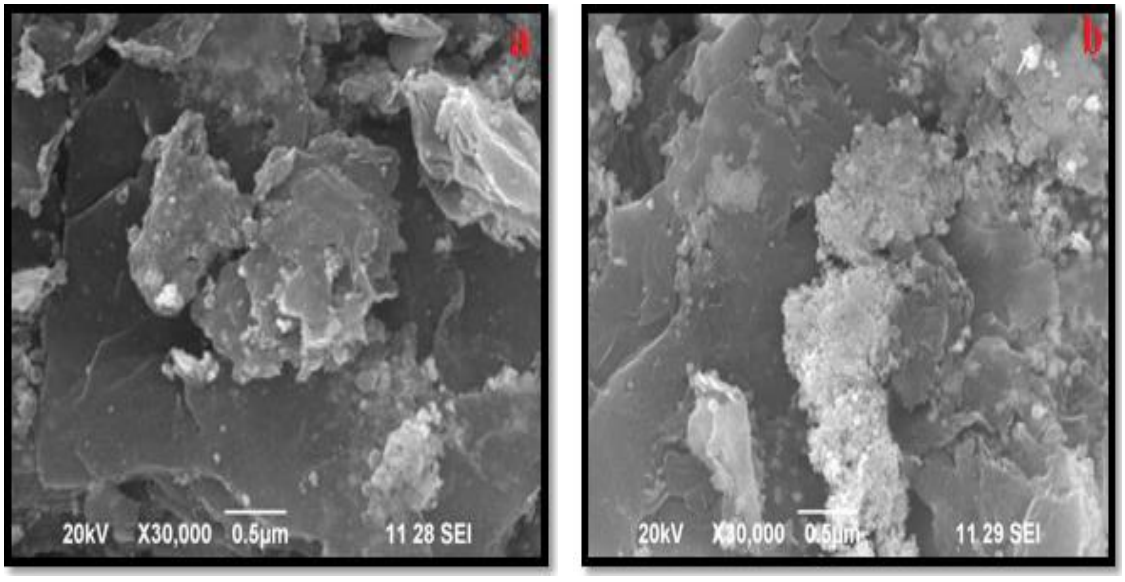

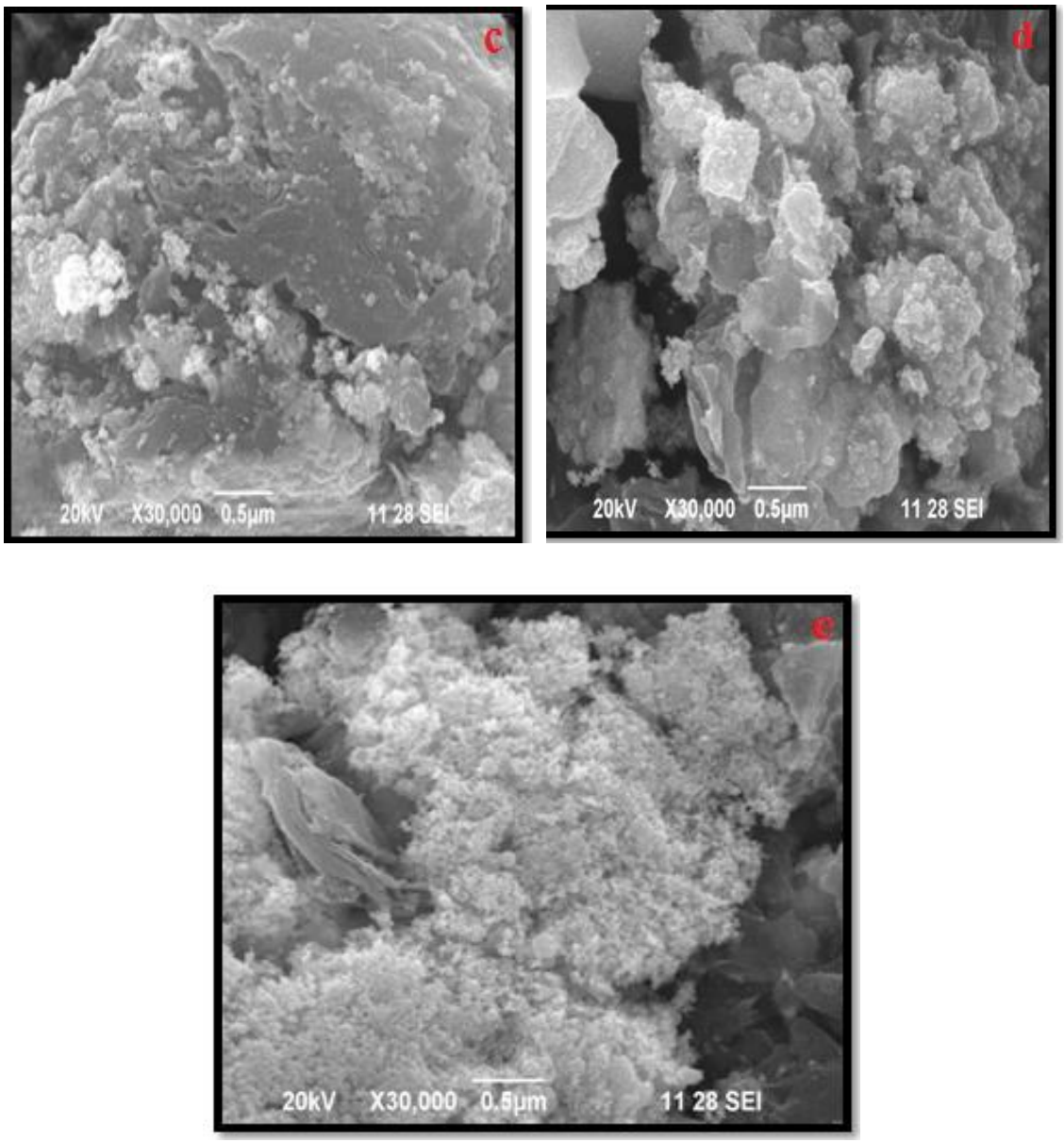

Figure.5.3. SEM images of gold nanoparticles encapsulated β-cyclodextrin functionalized reduced graphene oxide nanosheets using (a) 0.002 M (b) 0.004 M (c) 0.006 M (d) 0.008 M and (e) 0.01 M concentration of gold (III) chloride trihydrate

Figure.5.3.(a-e) shows the SEM images of the different concentrations ((0.002 M, 0.004 M, 0.006 M, 0.008 M and 0.01M) of rGONS/β-CD/Au nanocomposites. The SEM images of the synthesized nanocomposites shows that the gold nanoparticles are well anchored and uniformly distributed onto the surface of wrinkled rGO/β-CD nanosheets and are found to be spherical in shape [14] [17]. It is also observed that the distribution of gold nanoparticles on the surface of rGO/β-CD nanosheet is uniform for

the concentrations of rGO/β-CD/Au nanocomposites from 0.002 M to 0.006 M [18]. This may be due to the fact that the functionalities of oxygen groups on rGO/β-CD nanosheet enhances the overall negative zeta potential, thereby attracting positively charged gold nanoparticles. This encapsulation of gold nanoparticles with rGO/β-CD nanosheet enhances their degree of contact thereby suppressing the aggregation of Au nanoparticles and ensuring the greater stability [19]. This may also be due to the decrease in the surface energy of gold nanoparticles by the chemically functionalized β-cyclodextrin polymer on the surface of rGO nanosheets [20]. With the further increase in the concentrations from 0.008 M to 0.01 M, the encapsulation of gold nanoparticles on the surface of rGO/β-CD nanosheet is not uniform and tends to aggregate, that depicts the enhancement in the crystallite size, surface energy and mobility of gold nanoparticles encapsulated on the surface of rGONS/β-CD, which could also be evidenced from XRD and EDAX analysis. It is revealed from the morphological studies that the rGONS/β-CD/Au nanocomposite synthesized using 0.006 M concentration of gold (III) chloride trihydrate have large number of highly dispersed gold nanoparticles, which thereby minimizes the electro transfer barrier distance between the layers of rGONS and enhances the electrochemical property of the synthesized nanocomposites towards the detection of nitrophenol isomers [17].

5.3.4. EDAX ANALYSIS

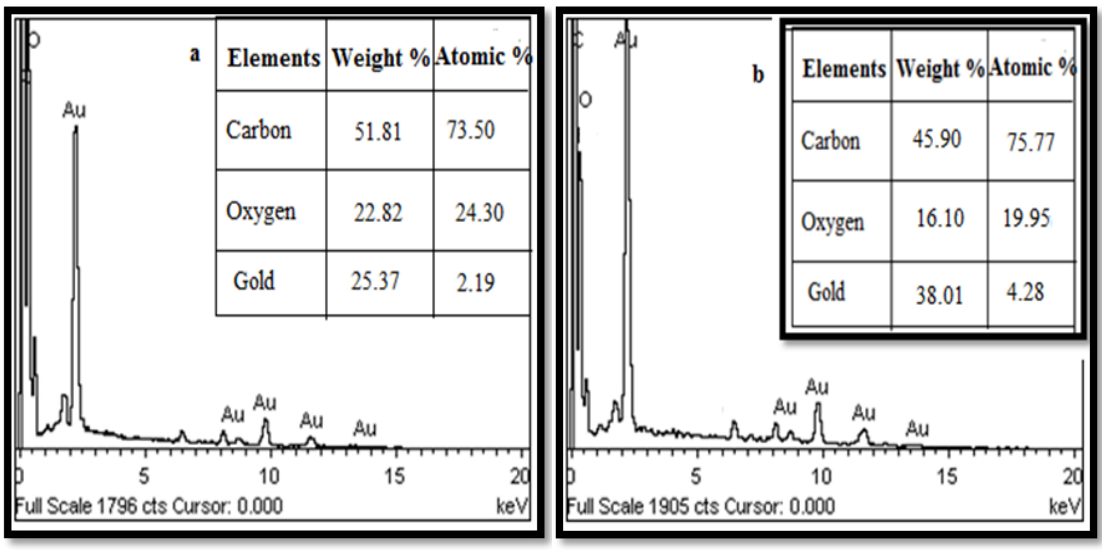

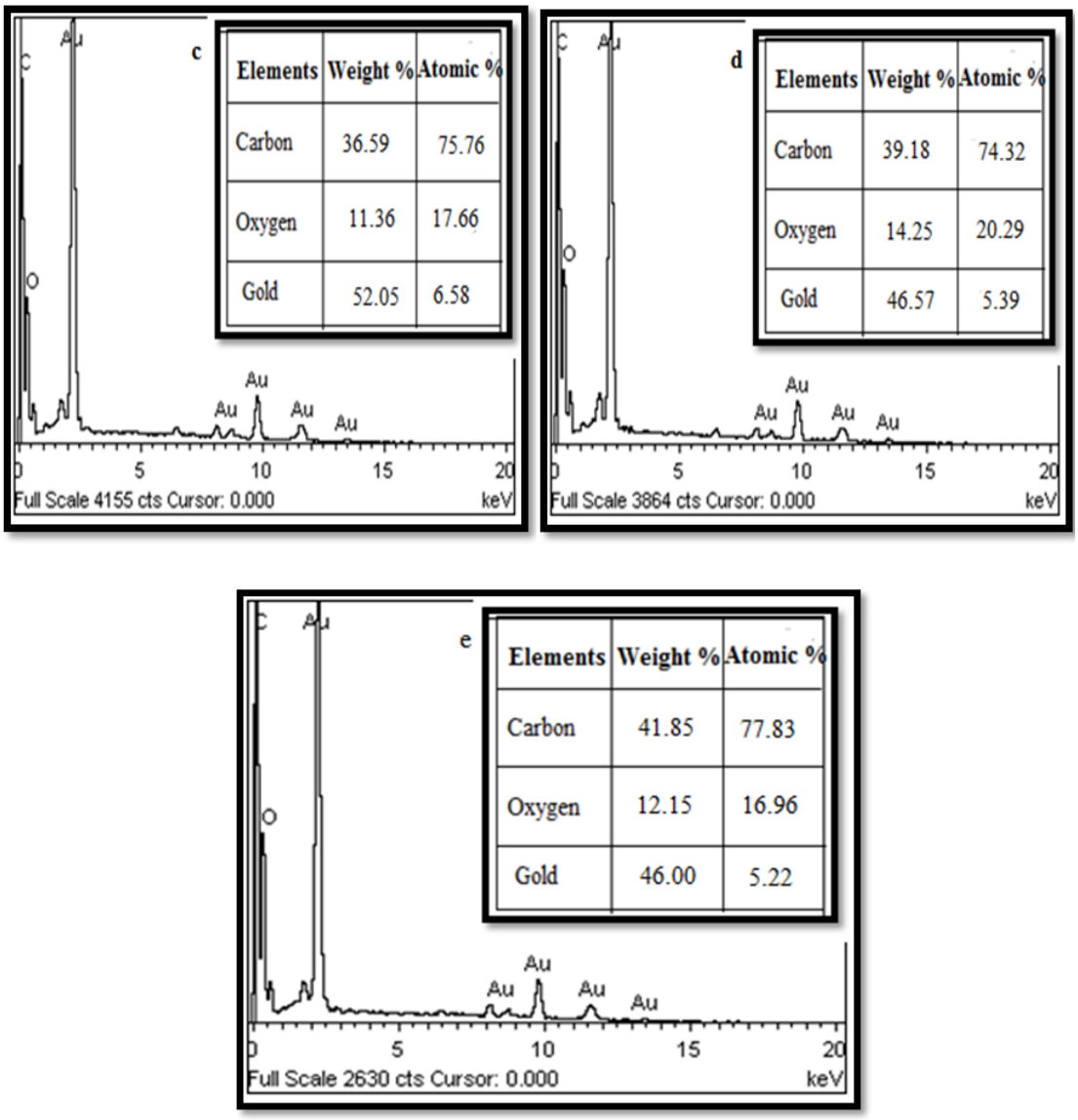

Figure.5.4. EDAX spectra of gold nanoparticles encapsulated β-cyclodextrin functionalized reduced graphene oxide nanosheets using (a) 0.002 M (b) 0.004 M (c) 0.006 M (d) 0.008 M and (e) 0.01 M concentration of gold (III) chloride trihydrate

Figure.5.4.(a-e) shows the EDAX spectra of five different concentrations (0.002 M, 0.004 M, 0.006 M, 0.008 M and 0.01 M) of rGONS/β-CD/Au nanocomposites. It reveals the presence of elements like carbon, oxygen and gold in the synthesized rGONS/β-CD/Au nanocomposites which confirms the successful synthesis of rGONS/β-CD/Au nanocomposites [14] [18]. The atomic and weight percentage of elements such as carbon, oxygen and gold existed in the synthesized rGONS/β-CD/Au nanocomposites is tabulated and shown in the inset of the Figure.5.4.(a-e). It is observed

from the inset of the Figure 5.4 that the presence of gold nanoparticles on the surface of rGO/β-CD nanosheet is found to be increased with the increase in the concentrations of gold precursor from 0.002 M to 0.006 M [18-19]. With the further increase in the concentration of gold (III) chloride trihydrate from 0.008 M to 0.01 M, the concentration of gold nanoparticles on the surface of rGONS/β-CD decreases, which could also be confirmed by SEM and XRD analysis [21].

5.3.5. HRTEM ANALYSIS

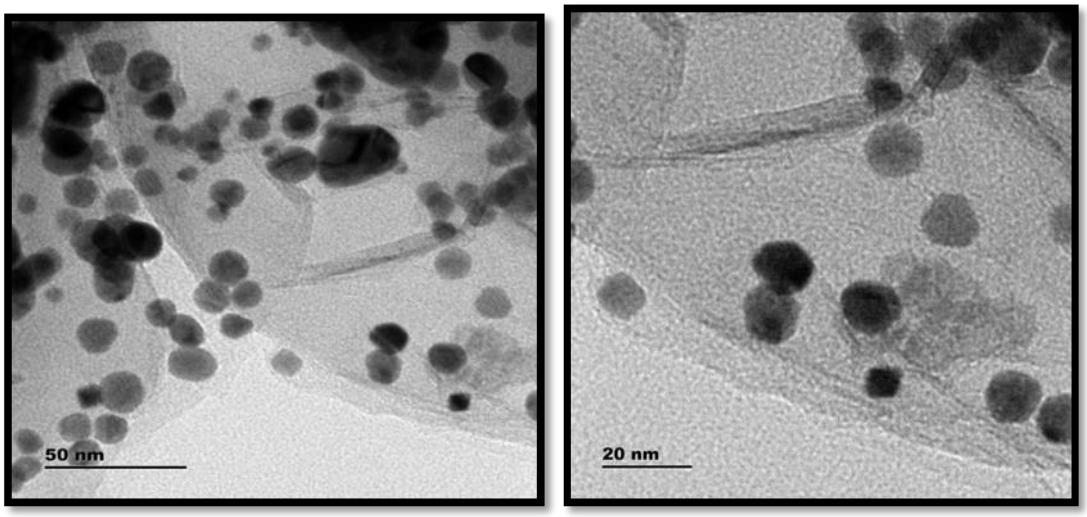

Figure.5.5. HRTEM images of gold nanoparticles encapsulated β-cyclodextrin functionalized reduced graphene oxide nanosheets using 0.006 M concentration of gold (III) chloride trihydrate

The structural and SEM analysis confirms that the rGONS/β-CD/Au nanocomposite synthesized using 0.006 M of gold (III) chloride trihydrate shows the good morphological behaviour with smaller crystallite size and hence it is further characterized using high resolution transmission electron microscope analysis.

Figure 5.5 shows the high resolution transmission electron microscopy images of the synthesized rGONS/β-CD/Au nanocomposites of 0.006 M concentration of gold precursor. The HRTEM image clearly shows the wrinkled morphology of β-cyclodextrin functionalized reduced graphene oxide nanosheets [22] and are decorated with spherical shaped gold nanoparticles [14]. This indicates efficient exfoliation of rGO nanosheets and good dispersibility of gold nanoparticles. These gold nanoparticles on the rGO/β-CD nanosheets appear as a dark spots with a particle size in

the range of 15 nm, which is in good agreement with XRD analysis. It is also observed from the TEM images that the gold nanoparticles are well incorporated on the surface and inside of rGO/β-CD nanosheets without agglomeration, which may be due to the presence of β-cyclodextrin molecules that acts as a stabilizing agent [15].

5.3.6. SAED ANALYSIS

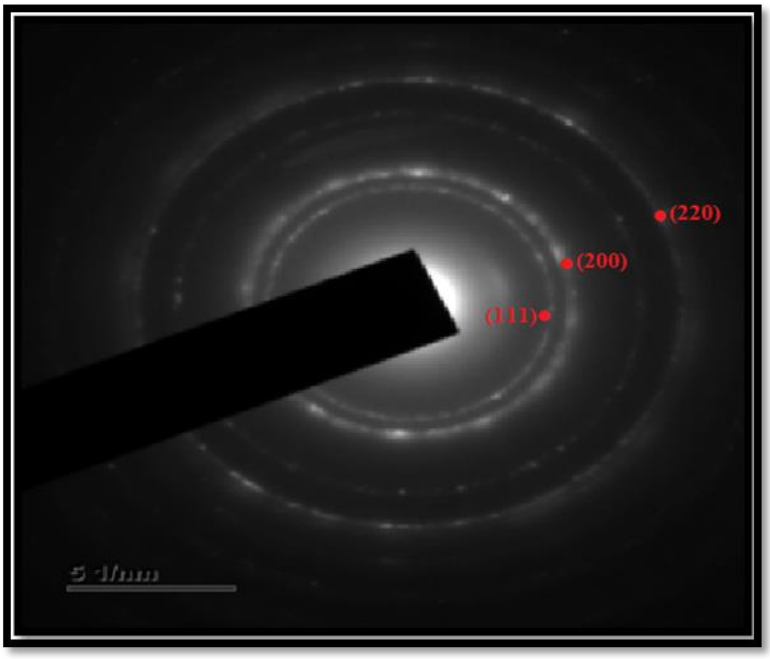

Figure.5.6. SAED pattern of gold nanoparticles encapsulated β-cyclodextrin functionalized reduced graphene oxide nanosheets using 0.006 M concentration of gold (III) chloride trihydrate

Selected area electron diffraction pattern of synthesized gold nanoparticles encapsulated β-cyclodextrin functionalized reduced graphene oxide nanosheets using 0.006 M concentration of gold (III) chloride trihydrate is shown in the Figure.5.6. The rings obtained in the SAED patter of the synthesized rGONS/β-CD/Au nanocomposite confirm the formation of high crystalline gold nanoparticles encapsulated rGO/β-CD nanosheets. The ring pattern obtained in the SAED results are well matched with the (111), (200) and (220) crystalline planes of face centred cubic phase of gold nanoparticles decorated on the rGO/β-CD nanosheets, which is consistent with the XRD analysis [14].

5.4. ELECTROCHEMICAL BEHAVIOUR OF MODIFIED ELCTRODES

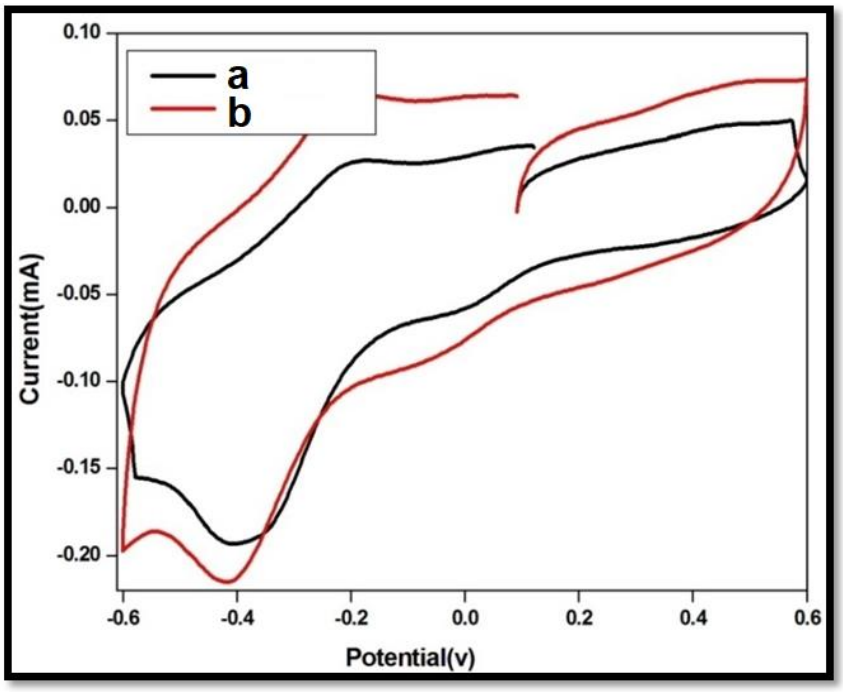

Figure.5.7.Cyclic voltagramm of 280 µM of o-NP at the (a) rGONS/Au/GCE (b) rGONS/β-CD/Au/GCE in 0.1 M PBS solution at the scan rate of 10 mV/s

Figure.5.7.(a & b) shows the cyclic voltagramm for the electrochemical behaviour of 280 µM of ortho-nitrophenol (o-NP) for gold nanoparticles encapsulated reduced graphene oxide nanosheets (rGONS/Au) modified GCE (curve a) and gold nanoparticles encapsulated β-cyclodextrin functionalized reduced graphene oxide nanosheets (rGONS/β-CD/Au) modified GCE (curve b) in a phosphate buffer solution (0.1 M, pH 6.0) at the scan rate of 10 mV/s. Here, the concentration of ortho-nitrophenol in the PBS medium is varied from 100 µM to 290 µM and the maximum redox peak current is obtained for the 280 µM of o-NP and are shown in the Figure.5.7.(a & b). The cyclic voltagramm of o-NP at the two modified electrodes shows the well defined reduction and oxidation peak which indicates that the electrochemical reaction of o-NP is completely reversible [12] [18] [23]. The rGONS/Au nanocomposite modified GCE shows the enhanced redox peak current for the 280 µM of o-NP with the peak current value of -0.19 mA, +0.02 mA as compared with that of the electrochemical behaviour of rGONS/GCE and rGONS/β-CD/GCE as discussed in the chapter 3. This may be due to the excellent electrocatalytic activity and large surface area of gold nanoparticles and rGO nanosheets and thus enhances the

electron transfer rate between the layers of rGONS [12] [13] [23]. The redox peak current for the rGONS/β-CD/Au/GCE (curve b) of 280 μM of ortho-nitrophenol is -0.22 mA and +0.07 mA, which is higher than that of the rGONS/Au/GCE. This might be attributed to the impact of high inclusion complexes, host-guest recognition and enrichment capability properties of β-CD polymer towards the electrocatalytic detection of o-NP [13]. In addition to this, the rGO nanosheets and gold nanoparticles provides large surface to volume ratio to enhance the loading amount of ortho-nitrophenol on the electrode surface [13]. The enhancement in the electrocatalytic reduction current of o-NP may also be due to the good synergistic effect between rGONS, β-CD and gold nanoparticles provides possible matrix to interact more number of o-NP molecules via intermediate hydrogen bond between O-H group of rGONS/β-CD [18] [12].

Hence it is revealed that the glassy carbon electrode (GCE) modified using rGONS/β-CD/Au nanocomposite could generate sufficient electron-transfer microenvironment to increase the electron transfer between o-NP and electrode surface under diffusion conditions to achieve the ultrasensitive detection of nitrophenol isomers than the other modified electrodes [13] [18].

5.5. ELECTROCHEMICAL DETECTION OF NITROPHENOL ISOMERS

The electrocatalytic activity toward the detection of ortho-, para- and meta-nitrophenol isomers are studied using various concentration of synthesized rGONS/β-CD/Au nanocomposite, various pH values of PBS medium and various potential scan rates and the results are presented in the following sections. For the optimization of various electrochemical parameters, the concentration of nitrophenol isomers in the electrolyte medium is varied and the results are given only for the concentration of nitrophenol isomers with maximum redox peak current.

5.5.1. Effect of rGONS/β-CD/Au concentration on electrocatalytic activity

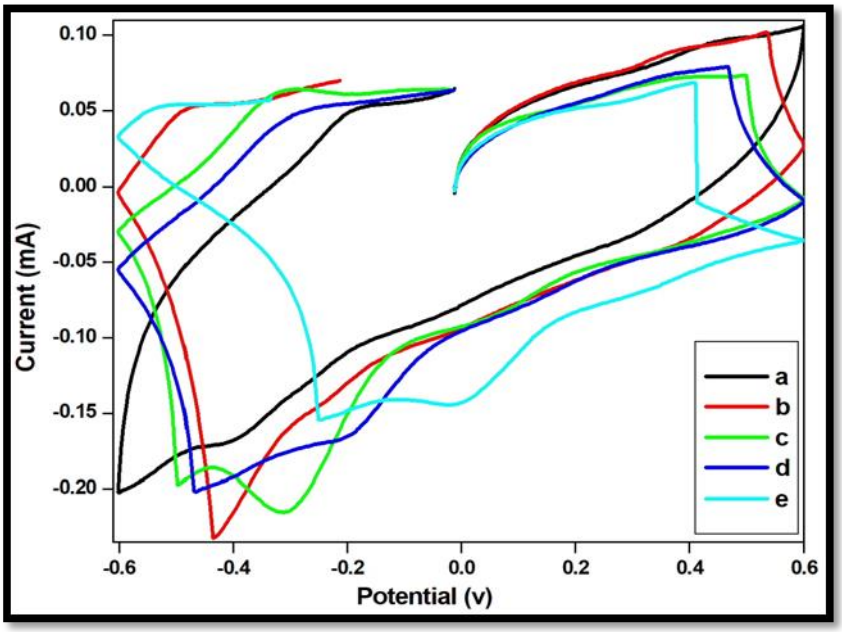

Figure.5.8. Cyclic voltagramm of 280 µM of o-NP at (a) 0.002 M (b) 0.004 M (c) 0.006 M (d) 0.008 M and (e) 0.01 M of gold nanoparticles encapsulated β-cyclodextrin functionalized reduced graphene oxide nanosheets in PBS solution

The influence of various concentration (0.002 M, 0.004 M, 0.006 M, 0.008 M and 0.01 M) of gold nanoparticles encapsulated β-cyclodextrin functionalized reduced graphene oxide nanosheets (rGONS/β-CD/Au) towards the electrochemical detection of 280 µM of ortho-nitrophenol is investigated and the results are shown in the Figure.5.8.(a-e). The modified glassy carbon electrode (GCE) is prepared individually by using 0.002 M, 0.004 M, 0.006 M, 0.008 M and 0.01 M concentration of rGONS/β-CD/Au nanocomposites and investigated in a 0.1 M of phosphate buffer solution at the

scan rate 10 mV/s. The current response towards the detection of ortho-nitrophenol is not prominent for the lower concentration such as 0.002 M and 0.004 M of rGONS/ β-CD/Au modified GCE and is found to be -0.15 mA and -0.166 mA respectively as shown in the Figure.5.8.(a and b). But with the increase in the concentration of rGONS/β-CD/Au nanocomposites modified GCE from 0.004 M to 0.006 M, a prominent electrocatalytic reduction peak is observed with the maximum current response of about -0.21 mA. This may be due to the presence of large amount of gold nanoparticles encapsulated on the surface of rGO/β-CD nanosheets which is most favourable for the electron conduction [12]. Further increase in the concentration of rGONS/β-CD/Au nanocomposites from 0.008 M to 0.01 M, the current response towards the detection of o-NP gradually decreases with the value of -0.164 mA and -0.142 mA and this may be due to the increased electron transfer resistance [13]. This phenomenon illustrates that, even though the gold nanoparticles could able to increase the conductivity of the electrode as the concentration of gold nanoparticles on the surface of rGONS/β-CD is too large, but as the concentration of gold nanoparticles employed to modify the surface of GCE becomes excessive, which makes the electron transfer more difficult and thereby decreases the electrode conductivity with the ortho-nitrophenol [12-13].

It is revealed from the electrochemical analysis that the electrochemical detection current response towards the 280 μM of o-NP is as $I_{pc,0.002\ M} < I_{pc,0.004\ M} < I_{pc,0.006\ M} > I_{pc,0.008\ M} > I_{pc,0.001\ M}$. The influence of concentration of gold nanoparticles on the electrochemical behaviour of rGONS/β-CD/Au nanocomposite towards the detection of o-NP is studied. The rGONS/β-CD/Au nanocomposite synthesized using 0.006 M concentration of gold (III) chloride trihydrate is chosen as an optimal electrode modifying material for the electrocatalytic detection of other nitrophenol isomers such as para- and meta-nitrophenol.

5.5.2 Effect of electrolyte pH

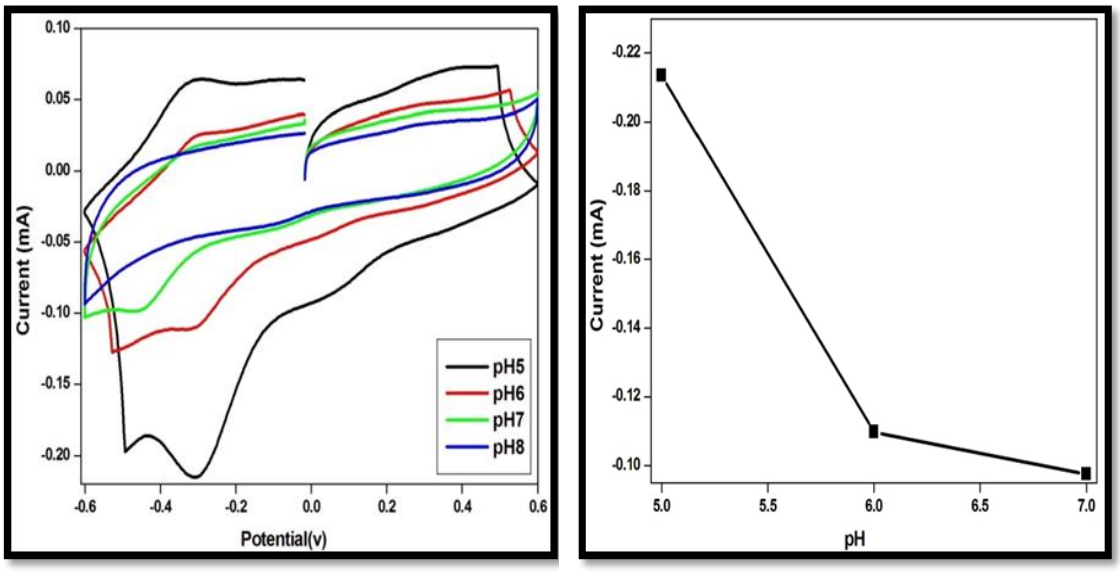

(a)

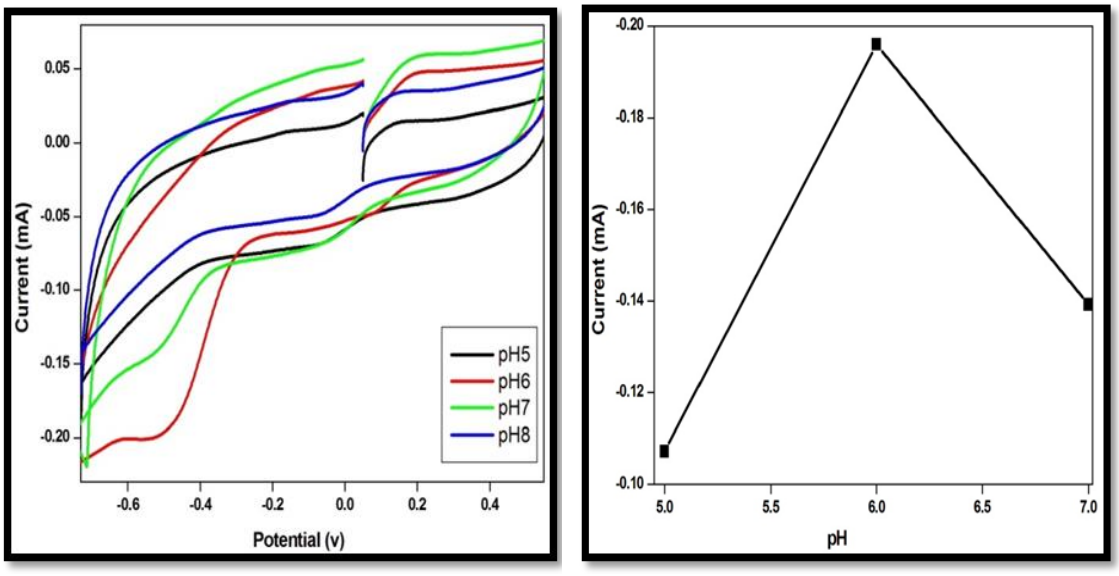

(b)

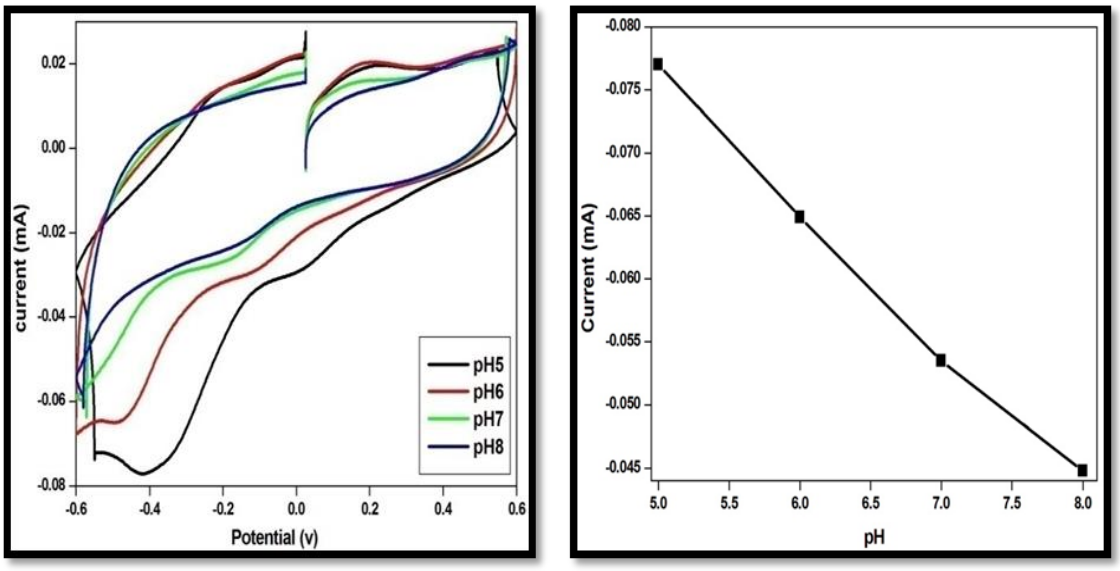

(c)

Figure.5.9. Effects of pH on the reduction peak current of (a) 280 µM o-NP and its linearity (b) 210 µM p-NP and its linearity (c) 220 µM m-NP and its linearity in 0.1M of PBS solution at the scan rate of 10 mV/s

In most of the electrochemical sensor investigation, the pH of an electrolyte medium is an important parameter. The effect of pH values of phosphate buffer solution (PBS) on the electrochemical reduction potential of ortho-, para- and meta-nitrophenol in the pH ranges from 5.0 to 8.0 using 0.006 M rGONS/β-CD/Au nanocomposites modified GCE at the scan rate of 10 mV/s and the calibration graph between pH and the corresponding current response is shown in the Figure.5.9 (a, b and c), respectively. It clearly shows that with the increase in the pH values of phosphate buffer solution from 5.0 to 8.0, the reduction and oxidation peak potential corresponding to the ortho-, para- and meta-nitrophenol isomers are shifted to negative and positive values respectively. This implies that the electrode reactions for the detection of o-, p- and m-nitrophenol isomers are carried out by the electron participation [12-13]. The calibration graph of Figure.5.9.(a-c) clearly depicts that the peak current corresponding to the electrocatalytic reduction of ortho- and meta-nitrophenols are maximum for the electrolyte with the pH value of 5.0. With the continuous increase in the pH of PBS medium from 6.0 to 8.0, the peak current corresponding to the reduction of ortho- and meta-NP decreases which may due to the instability of o- and m-NP in high acidic conditions [23]. But in the case of detection of para-nitrophenol, the reduction peak

current increases firstly with pH of PBS medium from 5.0 to 6.0 and reaches the maximum detection current at the pH value of 6.0. With the further increase in the pH from 7.0 to 8.0 leads to decrease in the current response. It is observed that as the pH of PBS medium is above 7.0, it could repulse negatively charged composite modified electrode, thereby reduces the electrocatalytic redox response of nitrophenol isomers [18]. Hence, the optimized pH values of the PBS medium for the further electrochemical investigation on o-, p- and m-NP are 5.0, 6.0 and 5.0, respectively.

5.5.3. Effect of scan rate

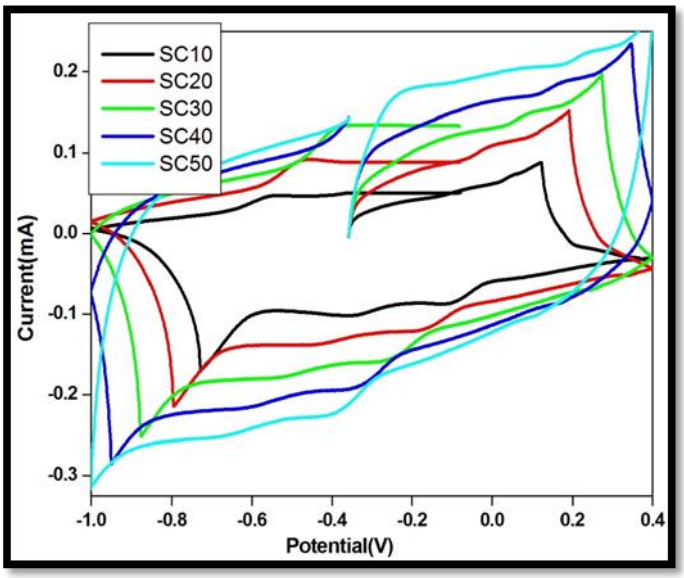

(a)

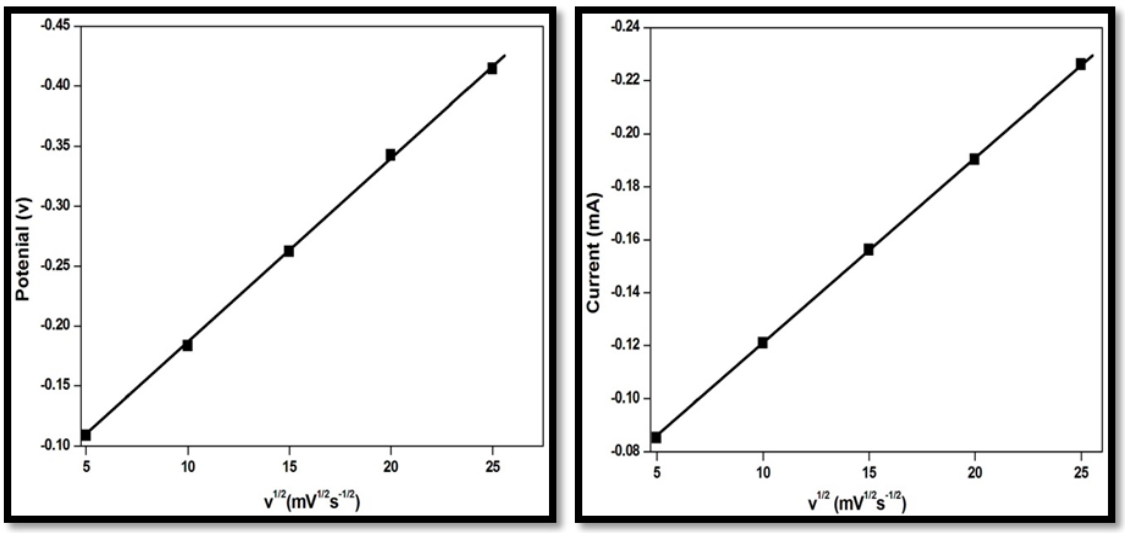

(b)

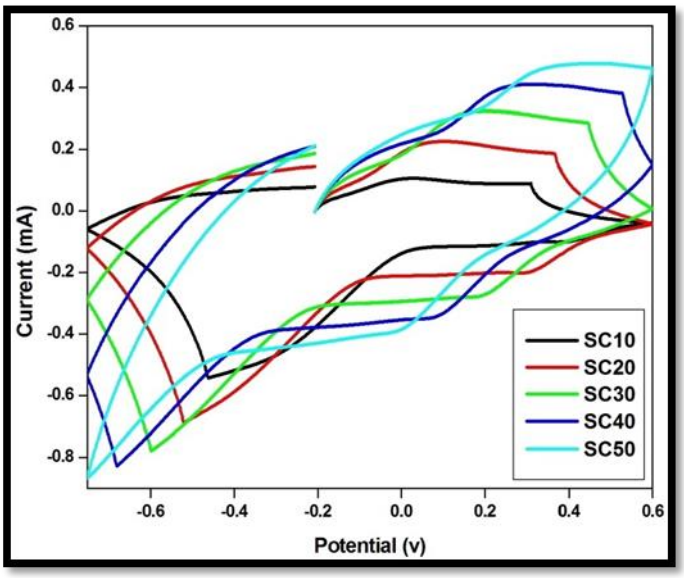
Current (mA)
Potential (v)
SC10
SC20
SC30
SC40
SC50

(c)

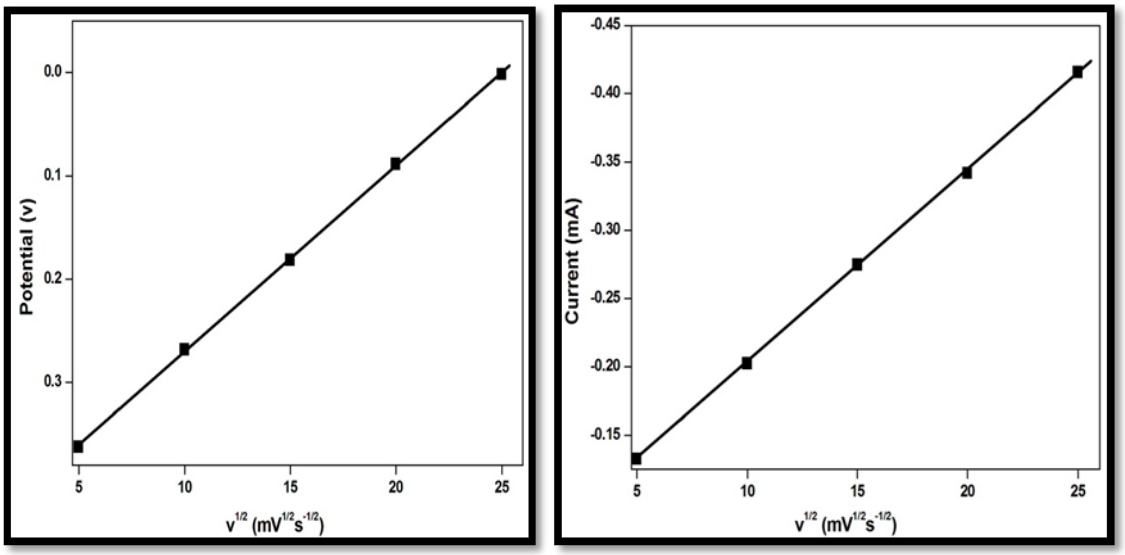
Potential (v)
v^1/2 (mV^1/2s^-1/2)
Current (mA)
v^1/2 (mV^1/2s^-1/2)

(d)

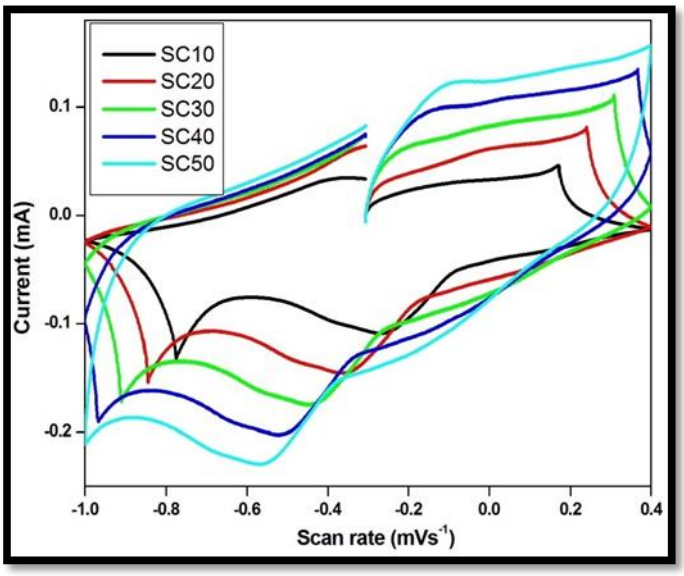

(e)

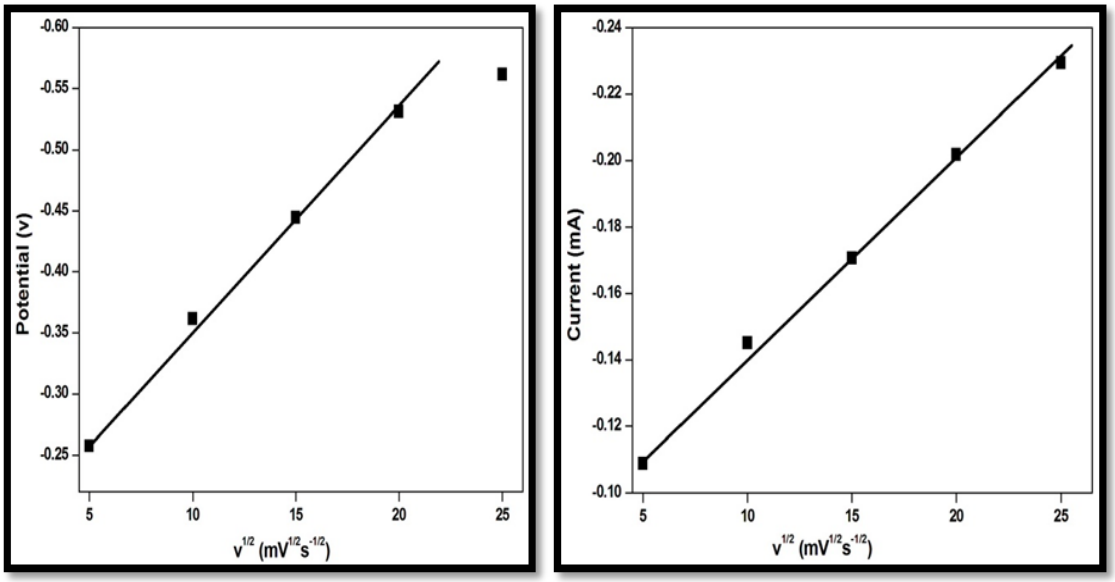

(f)

Figure.5.10. (a), (c) and (e) Effect of scan rate on the reduction current response for 280 µM, 210 µM, 210 µM of o-, p- and m-NP in 0.1 M PBS solution (b), (d) and (f) Linear relationship between E_{pa}, I_{pa} and square root of scan rate

Figure.5.10.(a, c and e) shows the cyclic voltagramm responses of 280 µM, 210 µM and 220 µM of ortho-, para- and meta nitrophenol isomers at 0.006 M of rGONS/β-CD/Au nanocomposite modified GCE under the influence of various scan

rates (10 to 50 mV/s) in 0.1 M of PBS solution (pH 5.0, 6.0 and 5.0) respectively. It is clearly observed from the Figure.5.10.(a, c and e) that the electrocatalytic reduction and oxidation peak potential of o-, p- and m-NP are shifted towards more negative and positive direction respectively with the increase of scan rate in the range of 10 to 50 mV/s [18]. The linearity graph shows that the reduction peak current of o-, p- and m-NP increases proportionally with the square root of the scan rate. A good linear relationship is observed in all the electrochemical detection process (o-, p- and m- NP), between the peak current and square root of the scan rate, thereby indicating that all three nitrophenol isomer compounds (o-, p-and m-NP) are electro-active under diffusion controlled processes [18].

5.5.4. Effect of analyte (o-, p- and m-NP) concentration

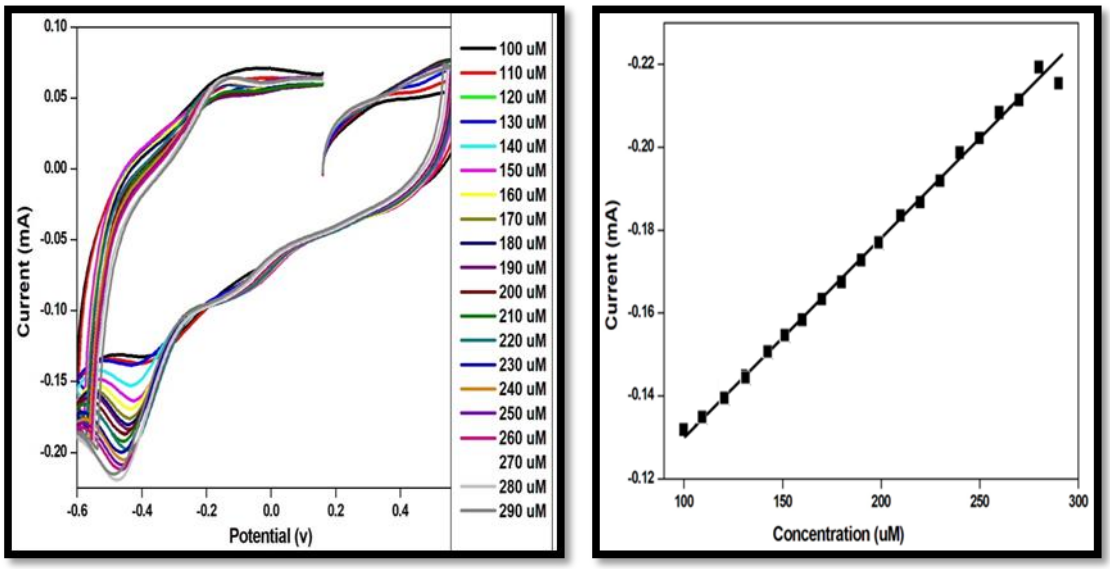

(a)

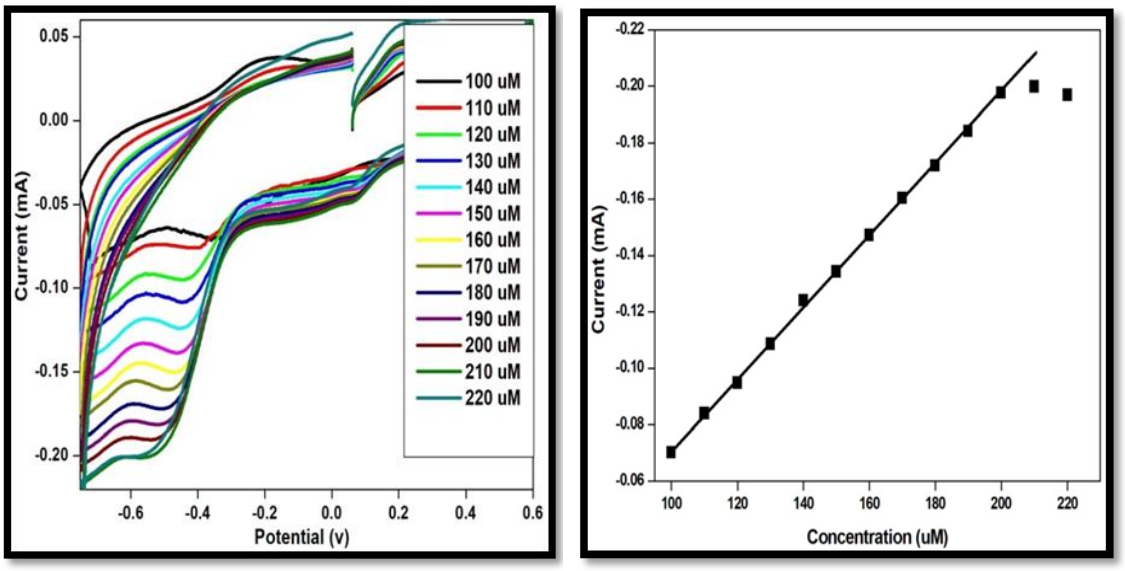

(b)

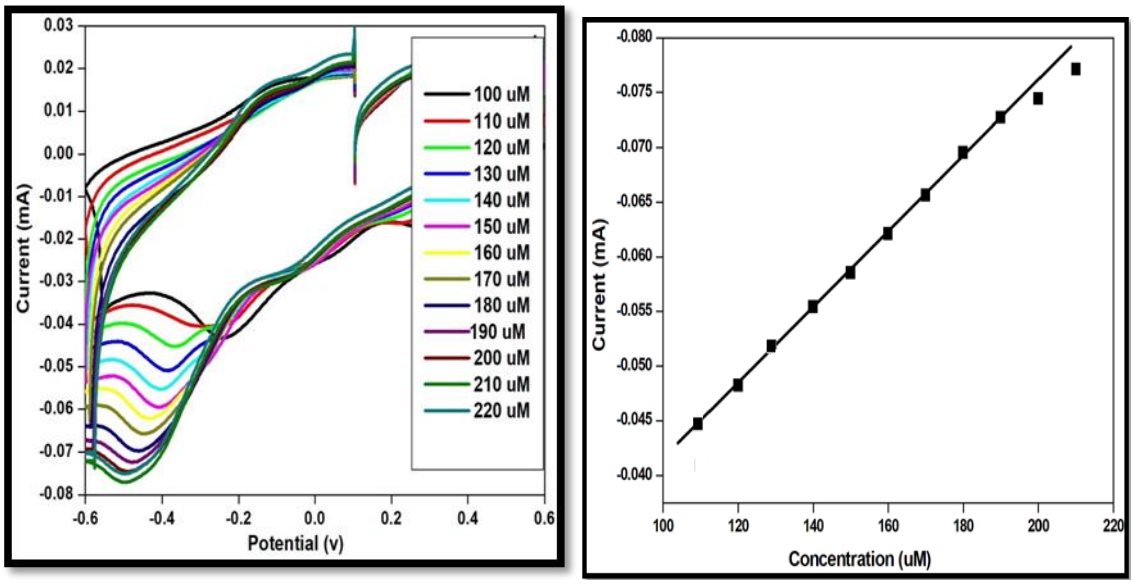

(c)

Figure.5.11. Cyclic voltagramm of rGONS/β-CD/Au/GCE in 0.1 M of PBS solution containing various concentrations of (a) o-NP, (b) p-NP and (c) m-NP

Figure.5.11.(a, b and c) shows the cyclic voltagramm of 0.006 M rGONS/ β-CD/Au nanocomposites modified GCE for the concentration of ortho-, para- and meta-nitrophenol varied from 100 µM to 290 µM, 100 µM to 220 µM and 100 µM to 220 µM in a PBS medium at the scan rate of 10 mV/s, respectively. The calibration graph is plotted between the different concentrations of ortho-, para- and

meta-nitrophenols and to their corresponding cathodic peak current and the results are shown in the Figure.5.11.(a-c). It is observed from the Figure.5.11.(a-c) that the electrocatalytic reduction capability of synthesized rGONS/β-CD/Au nanocomposite modified GCE for o-, p- and m-nitrophenols are from 100 μM to 280 μM, 100 μM to 210 μM and 110 μM to 210 μM respectively. With the further addition of another 10 μM of o-, p- and m-NP into the PBS medium, the cathodic peak current decreases. This result shows that the adsorption of o-, p- and m-nitrophenol sites on the surface of rGONS/β-CD/Au/GCE reaches its saturation state. The linear relationship between the cathodic peak current (mA) and concentration (μM) of three (o-, p- and m-NP) nitrophenol isomers are investigated using the calibration graph of Figure.5.11.(a-c) and are tabulated in the Table.5.1. The sensitivity of the rGONS/β-CD/Au nanocomposite modified GCE towards the detection of o-, p- and m-nitrophenol isomers are calculated using the calibration graph of Figure.5.11.(a-c) and the calculated values are listed in the Table.5.1.

Table.5.1. Linear range of detection and sensitivity value of the rGONS/β-CD/Au nanocomposite

Nitrophenol isomers	**Linear range of detection (μM)**	**Sensitivity ($mA\mu M^{-1}cm^{-2)}$**
Ortho-nitrophenol	100 to 280	8.87
Para-nitrophenol	100 to 200	1.92
Meta-nitrophenol	110 to190	1.02

It is confirmed from the Table.5.1 that the synthesized rGONS/β-CD/Au nanocomposite modified GCE shows a wide linear range of detection and a good sensitivity for the detection of ortho-nitrophenol. This may be due to the excellent synergistic effect of reduced graphene oxide nanosheets, gold nanoparticles and β-cyclodextrin towards the ortho-nitrophenol than the other two nitrophenol isomers.

5.6. CONCLUSION

A facile wet chemical methodology is applied for the synthesis of different concentrations (0.002 M, 0.004 M, 0.006 M, 0.008 M and 0.01 M) of gold nanoparticles encapsulated β-cyclodextrin functionalized reduced graphene oxide nanosheets (rGONS/β-CD/Au). The synthesized rGONS/β-CD/Au nanocomposites are employed as an efficient electrode modification material for the detection of nitrophenol isomers (o-, p- and m-NP) by electrochemical method. The structural analysis revealed that the crystallite size of the gold nanoparticles ranges from 9.16 nm to 9.20 nm for the concentration of 0.002 M to 0.006 M and there is an increase in the crystallite size from 9 nm to 12 nm for 0.008 M and 0.01 M and this may be due to the aggregation of gold nanoparticles encapsulated on the surface of rGONS/β-CD. The SEM analysis shows that the rGONS/β-CD/Au nanocomposite synthesized using 0.006 M concentration of gold (III) chloride trihydrate is uniformly decorated with large number of gold nanoparticles. The HRTEM analysis confirmed the formation of uniformly decorated spherical shaped gold nanoparticles on the surface of wrinkled cyclodextrin functionalized reduced graphene oxide nanosheets. The electrochemical analysis revealed that the synthesized rGONS/β-CD/Au nanocomposite shows a better linear range over the concentration from 100 μM to 280 μM with the sensitivity value of about 8.87 $mA\mu M^{-1}cm^{-2}$ for the detection of ortho-nitrophenol. Hence, the synthesized electrode material is better for the detection of ortho-nitrophenol than para- and meta-nitrophenol isomers.

References

1. A. Thabile Ndlovu, Omotayo Arotiba, W. Rui Krause, B. Bhekie Mamba, Electrochemical detection of o-nitrophenol on a poly (propyleneimine)-gold nanocomposite modified glassy carbon electrode, Int. J. Electrochem. Sci, 5, 1179-1186, (2010).

2. Honghong Rao, Weiming Guo, Huihui Hou, Hui Wang, Bo Yin, Zhonghua Xue, Guohu Zhao, Electroanalytical investigation of p-nitrophenol with dual electroactive groups on a reduced graphene oxide modified glassy carbon electrode, Int. J. Electrochem. Sci. 12, 1052-1063, (2017).

3. Weilu Liu Cong Li, Yue Gu, Liu Tang, Zhiquan Zhang, Ming Yang, One-step synthesis of β-cyclodextrin functionalized graphene/Ag nanocomposite and its application in sensitive determination f 4-nitrophenol, Electroanalysis, 25, 1-10, (2013).

4. Zhaona Liu, Junguo Du, Cuicui Qiu, Lihui Huang, Houyi Ma, Dazhong Shen, Yi Ding, Electrochemical sensor for detection of p-nitrophenol based on nanoporous gold, Electrochemistry Communications, 11, 1365-1368, (2009).

5. M. Mohammed Rahmana, M. Hadi Marwania, K. Faisal Algethami, M. Abdullah Asiria, A. Salem Hameed, Basma Alhogbi, Ultra-sensitive p-nitrophenol sensing performances based on various Ag_2O conjugated carbon material composites, Environmental Nanotechnology, Monitoring & Management, 8, 73-82, (2017).

6. Chao Zhang, Saravanan Govindaraju, Krishnan Giribabu, Yun Suk Huh, Kyusik Yun, AgNWs-PANI nanocomposite based electrochemical sensor for detection of 4-nitrophenol, Sensors and Actuators B, 252, 616-623, (2017).

7. Yujing Guo, Shaojun Guo, Jiangtao Ren, Yueming Zhai, Shaojun Dong, Erkang Wang, Cyclodextrin functionalized graphene nanosheets with high supramolecular recognition capability: synthesis and host-guest inclusion for enhanced electrochemical performance, ACS Nano, 4, 4001-4010, (2010).

8. V. Ramalakshmi, J. Balavijayalakshmi, Investigation on embellishment of metal nanoparticles on graphene nanosheets and its sensing applications, 14, 1-14, (2018).

9. Ming Chen, Yang Meng, Wang Zhang, Jun Zhou, Ju Xie, Guowang Diao, Beta-cyclodextrin polymer functionalized reduced-graphene oxide: Application for electrochemical determination imidacloprid, Electrochimica Acta, 108, 1-9, (2013).

10. Lihui Tian, Li Liu, Yueyuan Li, Qin Wei, Wei Cao, Ultrasensitive sandwich-type electrochemical immunosensor based on trimetallic nanocomposite signal amplification strategy for the ultrasensitive detection of CEA, Scientific Reports, 6, (2016).

11. Zhiming Jiang, Guangyu Li, Mingxiao Zhang, A novel electrochemical sensor based on SH-β-cyclodextrin functionalized gold nanoparticles/reduced-graphene oxide nanohybrids for ultrasensitive electrochemical sensing of acetaminophen and ofloxacin, Int. J. Electrochem. Scim 12, 5157-5173, (2017).

12. Huawen Hu, H. John Xin, Hong Hu, Xiaowen Wang, Xinkun Lu, Organic liquids-responsive β-cyclodextrin-functionalized graphene-based fluorescence probe: label-free selective detection of tetrahydrofuran, Molecules, 19, 7459-7479, (2014).

13. Wen Chen, Yuting Jiang, Fei Xue, Tingting Zhang, Glassy carbon electrode modified with gold nanoparticles/thiol-β-cyclodextrin-graphene for the determination of nonylphenol, Int. J. Electrochem. Sci, 12 12019-12036, (2017).

14. Jian Tang, Lingling Zhang, Yun Liu, Jie Zhou, Guangqiang Han, Weihua Tang, Gold nanoparticles-β-cyclodextrin-chitosan-graphene modified glassy carbon electrode for ultrasensitive detection of dopamine and uric acid, Electroanalysis, 26, 1-9, (2014).

15. Balamurugan Thirumalraj, Chellakannu Rajkumar, Shen Ming Chen, Selvakumar Palanisamy, One-pot green synthesis of graphene nanosheets encapsulated gold nanoparticles for sensitive and selective detection of dopamine, Scientific Reports, 7, 41213, (2017).

16. Wenbei Zhang, Jiuli Chang, Jianhua Chen, Fang Xu, Feng Wang, Kai Jiang, Zhiyong Gao, Graphene-Au composite sensor for electrochemical detection of para-nitrophenol, Res Chem Intermed, 38, 2443-2455, (2012).

17. E.H. Umukoro, M.G. Peleyeju, J.C. Ngila, O. Arotiba, Photoelectrochemical degradation of orange II dye in wastewater at a silver-zinc oxide/reduced graphene oxide nanocomposite photoanode, RSC Adv, 6, 52868-52877, (2016).

18. Haiyan Zhao, Xueping Ji, Beibei Wang, Na Wang, Xianrui Li, Ruixing Ni, Jujie Ren, An ultra-sensitive acetylcholinesterase biosensor based on reduced graphene oxide-Au nanoparticles-β-cyclodextrin/Prussian blue-chitosan nanocomposites for organophosphorus pesticides detection, Biosensors and Bioelectronics, 65, 23-30, (2015).

19. Selvakumar Palanisamy, Kokulnathan Thangavelu, Shen-Ming Chen, Balamurugan Thirumalraj, Xiao-Heng Liu, Preparation and characterization of gold nanoparticles decorated on graphene oxide @ polydopamine composite: Application for sensitive and low potential detection of catechol, Sensors and Actuators B, 233, 298-306, (2016).

20. MartinPumera, Graphene in biosensing, Materials today, 14, 308-315, (2011).

21. Dandan Su, Yuanyuan Zhang, Zhijie Wang, Qijin Wan, Nianjun Yang, Decoration of graphene nano platelets with gold nanoparticles for voltammetry of 4-nonylphenol, Carbon, 117, 313-321, (2017).

22. R. Manash Das, K. Rupak Sarma, Ratul Saikia, S. Vinayak Kale, V. Manjusha Shelke, Pinaki Sengupta, Synthesis of silver nanoparticles in an aqueous suspension of graphene oxide sheets and its antimicrobial activity, Colloids and Surfaces B: Biointerfaces, 83, 16-22, (2011).

23. Qiong Xue, Zhiguang Liu, Yujing Guo, Shaojun Guo, Cyclodextrin functionalized graphene–gold nanoparticles hybrids with strong supramolecular capability for electrochemical thrombin aptasensor, Biosensors and Bioelectronics, 68, 429-436, (2015).

24. Xianqing Tian, Changming Cheng, Hongyan Yuan, Juan Du, Dan Xiao, Shunping Xie, Martin M.F. Choi, Simultaneous determination of l-ascorbic acid, dopamine and uric acid with gold nanoparticles-β-cyclodextrin–graphene-modified electrode by square wave voltammetry, Talanta, 93, 79-85, (2012).